Two-photon processes in the presence of phase- or frequency-telegraph noise: Experimental study

R. Boscaino and R. N. Mantegna
Istituto di Fisica dell'Università degli Studi, Via Archirafi 36, I-90123 Palermo, Italy
(Received 15 December 1988)

Stochastic fields with non-Gaussian Markovian phase or frequency jumplike noise are produced at microwave frequency and used to induce two-photon (TP) processes in a $S=\frac{1}{2}$ spin system. The influence of the field statistics on the TP-induced second-order response is experimentally investigated in a system with very short relaxation times, in its stationary state and in the weak-field limit. In the case of frequency-telegraph noise the experimental spectra of the nonlinear response are found to reproduce roughly the spectral profiles of the corresponding driving fields but with a larger width. When the telegraph noise modulates the phase of the field, the relationship between input and output spectra depends on the phase-jump amplitude ϕ_0. For $\phi_0=\pi/4$ the spectrum of the response is much broader than the input one, whereas it is much narrower for $\phi_0=\pi/2$. The experimental results are interpreted using the calculation of the TP-induced second-order response worked out in the preceding paper [Boscaino and Mantegna, Phys. Rev. A **40**, 5 (1989)].

I. INTRODUCTION

In the preceding paper[1] (hereafter referred to as I) we investigated experimentally the two-photon (TP) processes induced in a two-level system by a phase-diffusion field,[2] namely by a field whose finite bandwidth originates in Gaussian Markovian fluctuations of its frequency. In this paper, the effect of the stochastic nature of the field on TP processes is studied for a different class of fields, whose statistical properties can be described in terms of jumplike noise.

Random-jump processes are widely used in atom-field interaction theories to take into account the time fluctuations of some interaction parameter. This may be either the atomic fequency or any variable (amplitude, frequency, or phase) characterizing the radiation. When the fluctuations occur in a time scale much shorter than the observational one, the time details of the individual events can be disregarded, and the fluctuations can be treated as instantaneous jumps between discrete values. A further simplification is to assume the noisy variable to be a Markov process,[3] in which case only the statistics of the jump occurrence and the distribution of the allowed values affect the interaction process under consideration.

Random-jump models of nonmonochromatic radiation are an attractive alternative to the phase-diffusion-field model.[2] In fact, jump models seem to be a more realistic picture of the field generated by a multimode source where mode hopping is the dominant broadening mechanism.[4] Moreover, they often permit nonperturbative examination of the atom-field interactions, as the atomic response functions can be evaluated exactly in finite terms.[5-8] For these reasons, a variety of models have been conceived in which a random-jump process modulates the phase, the frequency, or the amplitude of the field: bivalued and multivalued telegraph noise,[4-9] Kubo-Anderson processes,[10-12] independent-increment processes,[8,13] and shot noise.[14,15] Recently, non-Markovian jump models have been also considered which take into account an arbitrary degree of correlation between successive jumps.[16,17]

The influence of the jump noise of the field on the nonlinear response of two- and three-level systems has been considered for several strong-interaction phenomena, e.g., ac Stark effect,[10] multiphoton absorption,[15] resonance fluorescence,[4-9,13,17] and four-wave mixing.[16] In all these phenomena the atomic response depends strongly on the statistics of the assumed jump process and on the interplay between the characteristic time of the stochastic field and that of the system.

From an experimental point of view, efforts have been made recently to realize radiation sources with externally adjustable statistical properties to test theories of noisy interactions. This has been done successfully for the phase-diffusion field, both in optics and in the microwave region, in connection with experiments of TP absorption,[18] double optical resonance,[19] coherent transients,[20] and second-harmonic (SH) generation.[1,21] To our knowledge, similar experiments employing random-jump fields have not yet been reported.

In this paper we report on the realization of microwave fields whose spectra are broadened by jumplike noise. In particular we are concerned here with two kinds of fields, in which either the frequency or the phase is modulated by a bivalued random-telegraph noise (RTN). Bivalued RTN is the simplest example of random jump process; it is a non-Gaussian, Markovian process with a Poisson distribution of the number of jumps in a fixed time interval. At variance to a previous realization[22] of a RTN-modulated rf source, in our realizations both the jump excursion and the mean dwell time of the RTN can be varied externally.

In our experiments the RTN-modulated radiation, with a mean frequency $\bar{\omega}$, is used to drive a TP-resonant two-level ($S=\frac{1}{2}$) spin system. As in I, we study the effect of the field statistics on the TP-induced second-order response of the system by monitoring the radiation that it emits in a narrow spectral region centered at the second harmonic (SH) frequency $2\bar{\omega}$.[23] As known, frequency modulated by RTN (RTN-FM) and phase modulation by RTN (RTN-PM) are physically different from each other and are expected to yield different effects both on the driving field and on the atomic response. For RTN-FM of the driving field, we observe a two-peak or a single-peak SH emission spectrum depending on the parameter σT, where σ is the frequency jump and T is the mean dwell time of the RTN. We find that, for $\sigma T \ll 1$, the spectral width of the response is four times larger than the width of the input field, whereas, in the opposite limit $\sigma T \gg 1$, its peak-to-peak distance is twice the input one. For the RTN-PM case, we report the experimental results obtained for two values of the jump amplitude ϕ_0, $\phi_0 = \pi/4$ and $\phi_0 = \pi/2$. For this kind of field, the profile of the SH spectrum is found to be quite different from that of the driving field; in particular, for $\phi_0 = \pi/2$, it is much narrower than the input one.

In Sec. II we describe the properties of our RTN voltages. In Sec. III we report our method for generating RTN-FM and RTN-PM fields, analyze the statistics of the obtained fields, and report the experimental SH spectra. Finally, we make use of the semiclassical calculation of the second-order response worked out in I to interpret other experimental results.

II. RANDOM-TELEGRAPH NOISE VOLTAGES

We consider here a RTN voltage $v(t)$ with the following properties: (i) $v(t)$ can assume only two values with equal probability; (ii) $v(t)$ is constant except for instantaneous jumps between the two allowed values; (iii) $v(t)$ is a stationary Markovian process[3] characterized by the exponential density function $p(t_d)$ of the dwell time t_d:

$$p(t_d) = (1/T)\exp(-t_d/T) , \tag{1}$$

where T is the mean value of t_d. The probability $P(n,\tau)$ that its state changes n time in the interval τ is Poissonian

$$P(n,\tau) = \exp(-\tau/T)(\tau/T)^n/n! . \tag{2}$$

To obtain RTN voltage signals, computer-generated random-number sequences are preliminarily prepared. The starting point of our procedure is a sequence $\{x_n\}$ of random numbers uniformly distributed in the interval $0 < x_n < 1$. The transformation $y_n = -k \ln x_n$ yields a sequence $\{y_n\}$ of random numbers distributed in the interval $(0,\infty)$ with an exponential density function $P(y) = \exp(-y/k)$ and a mean value $\bar{y} = k$. Finally, $\{y_n\}$ is used to control the jumps of a random binary sequence $\{z_i,\ i=1,\ N_z = 30\,000\}$, where z_i is a two-value (0,1) variable changing its state $(z_i \neq z_{i-1})$ at $i = i_n$ with $i_n = i_{n-1} + \mathrm{int}(y_n)$.

A set of sequences $\{z_i\}$ prepared with different values of k is stored in the user memory of an arbitrary-waveform generator. On external command, the selected sequence $\{z_i\}$ is retrieved and repeatedly converted to an analog voltage: $v(t) = V_R z_i$ for $i\Delta t < t < (i+1)\Delta t$. V_R is an adjustable reference voltage and Δt is the conversion time step (minimum 40 ns). The resulting signal $v(t)$ jumps back and forth between 0 and V_R at random times $t_n = i_n \Delta t$, as in Fig. 1(a). The dwell time $t_d = t_n - t_{n-1} = \mathrm{int}(y_n)\Delta t$ has an exponential distribution with a mean value $T = k\Delta t$.

In Table I we list the parameters of the voltage signals used in the experiments described below. As shown, a wide range of T is covered from 1.78 to 100 μsec. To obtain a given T, the parameters k and Δt are so chosen as to minimize distortions of the statistics of $v(t)$. Actually $v(t)$ departs from an ideal RTN signal for two reasons. The former is the finite length of the generating sequence $\{z_i\}$, causing $v(t)$ to repeat after a period $T_R = N_z \Delta t$; the latter is the conversion time step Δt. As a consequence, dwell times outside the range Δt to $N_z \Delta t$ are cut out. For all the signals listed in Table I, the condition $50\Delta t \le T \le 0.01 T_R$ is fulfilled, which saves dwell times from $0.02T$ up to $100T$.

The statistical analysis of the obtained RTN signals $v(t)$ has been carried out by determining the density function $p(t_d)$ and the occurrence frequency $P(n,\tau)$. Typical results are reported in Figs. 1(b) and 1(c), as obtained for the RTN voltage A of Table I. The experimental histogram $p(t_d)$ in Fig. 1(b) has been determined with a time resolution of $T/5$ by counting how many times t_d falls within the range from $t_d - T/10$ to $t_d + T/10$ and normalizing to unit area; as shown in the figure, the exponential law of Eq. (1) with a decay time equal to the nominal T fits quite well the experimental data. In Fig. 1(c) the experimental values of $P(n,\tau)$ are plotted versus n, as obtained by scanning the same signal $v(t)$ with a window $\tau = 8\ \mu$ sec, counting how many times a number n of jumps occurs, and normalizing to units area; fair agreement is found between the experimental data and the Poisson distribution of Eq. (2) calculated with the nominal value of T. Similarly good agreement between experimental and theoretical data is found for all the signals listed in Tables I.

III. RTN-MODULATED FIELDS AND SECOND-ORDER RESPONSES

The RTN voltage signals $v(t)$, obtained as described above, are then used to realize nonmonochromatic microwave fields,

$$\mathbf{b}(t) = \mathbf{b}_1 \exp\{-i[\bar{\omega}t + \phi(t)]\} + \mathrm{c.c.} , \tag{3}$$

in which either the phase $\phi(t)$ or the instantaneous frequency deviation $\mu(t) = \dot{\phi}(t)$ is a bivalued RTN. In the following $S_1(\omega - \bar{\omega})$ denotes the power spectrum of $\mathbf{b}(t)$ and δ_1 its half width at half maximum (HWHM).

Apart from the statistics of the driving field, the experiments reported below are similar to those reported in I. So, here we limit ourselves to a brief outline, just to state the relevant experimental conditions. The field $\mathbf{b}(t)$ of Eq. (3) drives a system of N spins $S = \frac{1}{2}$ whose frequency is tuned to the TP resonance $\omega_0 = 2\bar{\omega}$ with the mean fre-

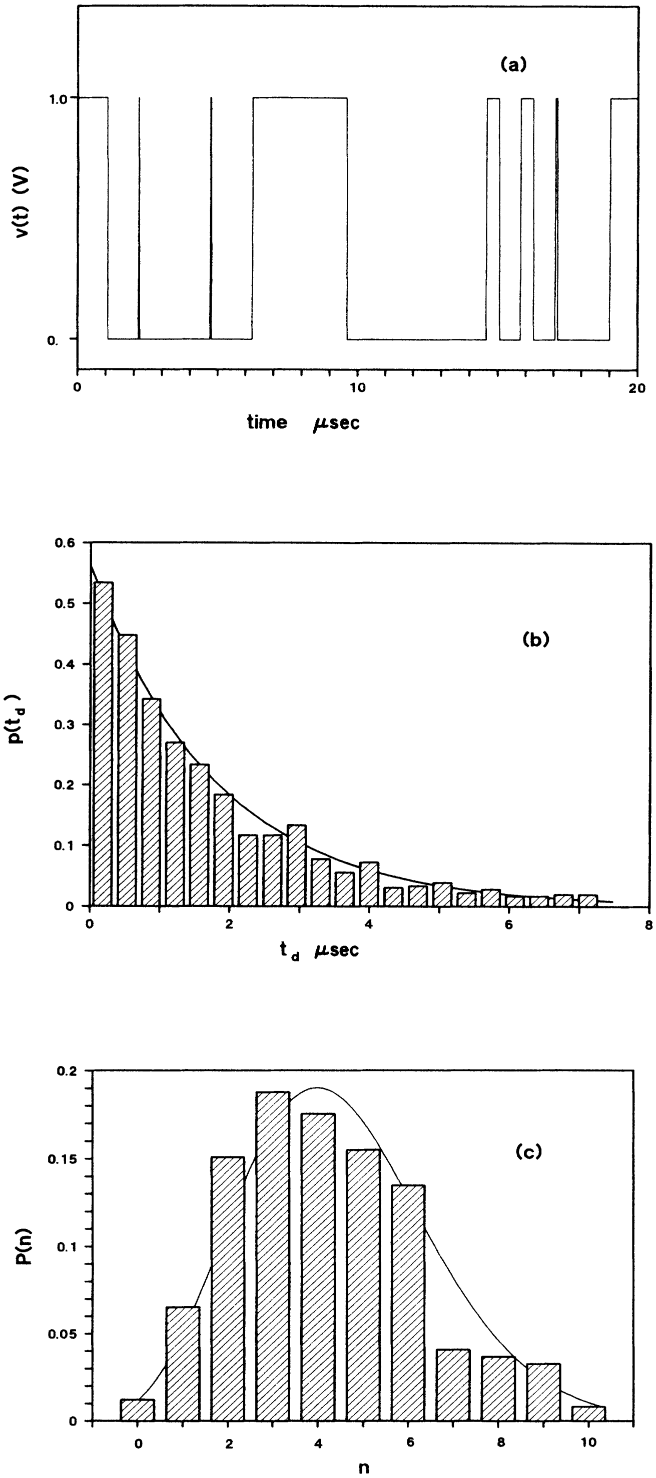

FIG. 1. Statistical analysis of the telegraph-noise voltage $v(t)$ indicated as A in Table I. (a) Time dependence of $v(t)$ in a window of 20 μsec. (b) Distribution function $p(t_d)$ (normalized to unit area) of the dwell time. The histogram is the result of the analysis of $v(t)$ and the curve is the exponential law of Eq. (1) with $T=1.78$ μsec. (c) The histogram shows the frequency of n jumps in intervals τ of 8.0 μsec in $v(t)$; the curve is the Poisson distribution of Eq. (2) with $T=1.78$ μsec.

TABLE I. Random-telegraph signals $v(t)$ used for generating RTN-FM and RTN-PM fields. T is the mean dwell time. N_j is the number of jumps in the repetition period T_R.

$v(t)$	T (μsec)	N_j	T_R (msec)	Resolution (nsec)
A	1.78	670	1.2	40
B	3.16	400	1.2	40
C	5.62	210	1.2	40
D	10.0	120	1.2	40
E	17.8	170	3.0	100
F	31.6	190	6.0	200
G	56.2	110	6.0	200
H	100.0	150	15.0	500

quency $\bar{\omega}$ of $b(t)$ ($\bar{\omega}=2\pi\times 2.95$ GHz). The Rabi frequency $\omega_R(t)$ of the TP transitions induced by $\mathbf{b}(t)$ is given by[24]

$$\omega_R(t)=\omega_{R0}\exp[i\phi_R(t)] , \tag{4}$$

with

$$\omega_{R0}=[\gamma^2 b_1^2 \sin(2\alpha)/\omega_0] \text{ and } \phi_R(t)=2\phi(t) .$$

Here γ is the gyromagnetic ratio and α is the polarization angle of $\mathbf{b}(t)$. Our experiments aim at investigating the effect of the field statistics on the TP-induced second-order response of the system, namely on its SH transverse magnetization $m_x^{(2)}(t)$. As calculated in I, the power spectrum $S_2(\omega-2\bar{\omega})$ of $m_x^{(2)}(t)$ images the spectrum $S_R(\omega)$ of $\omega_R(t)$:

$$S_2(\omega-2\bar{\omega})=\tfrac{1}{16}\hbar^2\gamma^2 N^2 T_2^2 S_R(\omega) , \tag{5}$$

where T_2 is the dephasing time of the system. We emphasize that Eq. (5) was derived for the steady-state response of a two-level system at TP resonance within the weak-field approximation and assuming that the correlation time of the input field is much longer than the relaxation times T_1 and T_2 of the system (in our sample and in our experimental conditions $T_1=T_2=0.07$ μsec).

The RTN-FM case and the RTN-PM one are considered separately in the following two subsections. For each case, first we examine the properties of the obtained field $\mathbf{b}(t)$ and then we report the corresponding experimental spectra of the SH radiation emitted by the system.

A. Frequency modulation

In this case the instantaneous frequency deviation $\mu(t)=\dot{\phi}(t)$ of $b(t)$ in Eq. (3) is a zero-mean RTN, jumping between σ and $-\sigma$. As known,[6,25] the power spectrum of $b(t)$ is given by

$$S_1(\omega-\bar{\omega})=\frac{8\pi b_1^2\sigma^2T^3}{(\omega-\bar{\omega})^4T^4+2T^2(\omega-\bar{\omega})^2(2-\sigma^2T^2)+\sigma^4T^4} . \tag{6}$$

Depending on σT, $S_1(\omega-\bar{\omega})$ can be either a singlet (for $\sigma T<\sqrt{2}$) or a doublet (for $\sigma T>\sqrt{2}$) with two symmetrical peaks at $\omega-\bar{\omega}=\pm(\sigma^2T^2-2)^{1/2}/T$. In both cases $S_1(\omega-\bar{\omega})$ is non-Lorentzian, as its far wings fall off as $1/(\omega-\bar{\omega})^4$. However, for $\sigma T \ll 1$, its center part is approximately described by a Lorentzian curve with a HWHM $\delta_1=(\sigma^2T)/2$. In the other limit $(\sigma T \gg 1)$ peak-to-peak distance tends to $\delta_{1\,\mathrm{p.p.}}=2\sigma$.

In order to produce this kind of radiation, one of the RTN signals of Table I added to a dc voltage $-V_R/2$ for symmetric excursion is used to drive the FM network of a microwave source. The source is a cavity-stabilized klystron oscillator tuned at $\bar{\omega}$; its FM circuit has a bandwidth of nearly 5 MHz and a voltage-to-frequency conversion $K_{\mathrm{VFC}}=50.5\pm0.5$ kHz/V, so that $\sigma=\frac{1}{2}K_{\mathrm{VFC}}V_R$. Representative spectra of the obtained radiation are shown in Fig. 2, for two different values of σT: the former 2(a) $(\sigma T=0.28)$ is a bell-shaped spectrum with $\delta_1/2\pi=3.4\pm0.3$ kHz; the latter 2(b) $(\sigma T=18.0)$ exhibits two peaks distant $\delta_{1\mathrm{p.p.}}/2\pi=98\pm4$ kHz. The smooth curves are the theoretical spectra calculated from Eq. (6) for nominal values of σ and T; as shown, for both the spectra, the agreement between experimental and theoretical spectra is remarkable, down to -60 dB below the maxima. Similarly good agreement is found at intermediate values of σT.

When a RTN-FM field is used to drive the TP-resonant spin system we find that the spectrum $S_2(\omega-2\bar{\omega})$ of the TP-induced second-order response of the system reproduce roughly the spectral profile of the input field, but with a larger width. The curves in Figs. 2(c) and 2(d) are the SH emission spectra measured when the radiation 2(a) and 2(b), respectively, is used as driving field. As shown, for $\sigma T=0.28$ the SH spectrum 2(c) has a bell-shaped form with a HWHM $\delta_2/2=14.5\pm1.5$ kHz, namely nearly four times larger than the input one: $\delta_2/\delta_1=4.3\pm0.4$. In the other case $(\sigma T=18)$ the SH spectrum 2(d) has a two-peak structure, with a peak-to-peak distance $\delta_{2\mathrm{p.p.}}/2\pi=194\pm4$ kHz, namely with $\delta_{2\mathrm{p.p.}}/\delta_{1\mathrm{p.p.}}=2.0\pm0.2$.

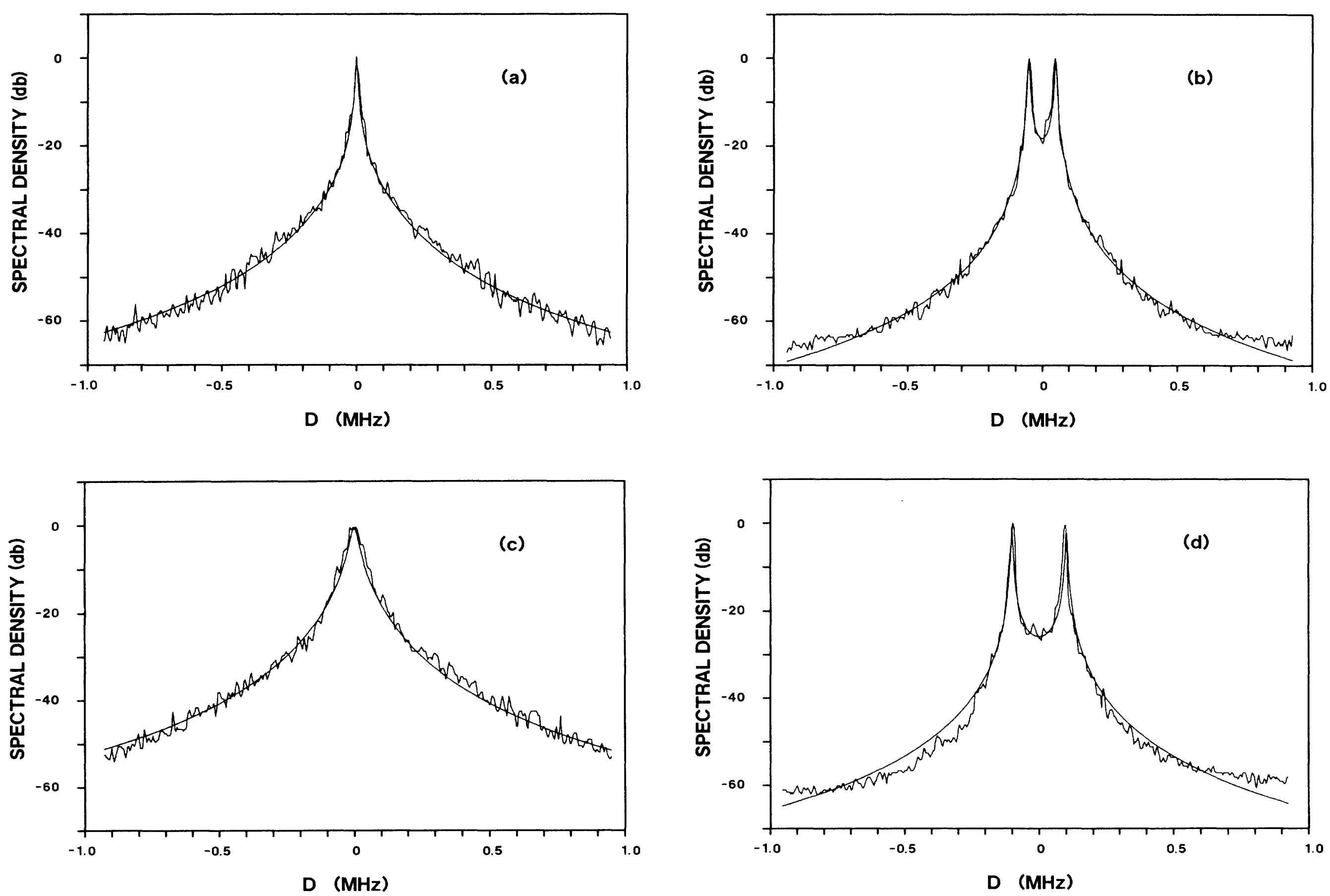

FIG. 2. Telegraph noise of the frequency. In (a) and (b) we report the experimental spectra of the driving field obtained for two different values of σT: $\sigma T=0.28$ (a) and $\sigma T=18.0$ (b). $D=(\omega-\bar{\omega})/2\pi$. These spectra are obtained by using the noise signals A and G of Table I, respectively; the HWHM of the spectrum (a) is $\delta_1/2\pi=3.4\pm0.3$ kHz, the peak-to-peak distance of the spectrum (b) is $\delta_{1\mathrm{p.p.}}/2\pi=98\pm4$ kHz. In (c) and (d) we report the experimental spectra of the second harmonic radiation emitted by the system when driven by the radiation (a) and (b), respectively. $D=(\omega-2\bar{\omega})/2\pi$. The HWHM of spectrum (c) is $\delta_2/2\pi=14.5\pm1.5$ kHz; the peak-to-peak distance of spectrum (d) is $\delta_{2\mathrm{p.p.}}/2\pi=194\pm4$ kHz. Smooth curves are theoretical spectra, calculated as described in the text.

The experimental results reported above are in agreement with the expected ones. In fact, for a RTN-FM field $b(t)$, $\omega_R(t)$ in Eq. (4) is a stochastic process whose instantaneous frequency $\dot{\phi}_R(t)=2\dot{\phi}(t)$ is as well a RTN, with the same dwell time but with a jump excursion twice larger $\sigma_R=2\sigma$. So, the spectrum $S_R(\omega)$ can be obtained in a straightforward way by rescaling Eq. (6). Finally, by using Eq. (5), we obtain

$$S_2(\omega-2\bar{\omega})=S_0\frac{\sigma^2T^3}{(\omega-2\bar{\omega})^4T^4+4T^2(1-2\sigma^2T^2)(\omega-2\bar{\omega})^2+16\sigma^4T^4}\ , \tag{7}$$

with

$$S_0=(\pi\hbar^2N^2\gamma^2/16)\omega_{R0}^2T_2^2\ .$$

The smooth curves in Figs. 2(c) and 2(d) are the spectra $S_2(\omega-2\bar{\omega})$ of Eq. (7) calculated with the nominal values of σ and T of the input field. As shown, the agreement with the experimental spectra is quite good, at least down to -40 dB below the maximum. Moreover, we calculate from Eq. (7) that for $\sigma T \ll 1$ the HWHM δ_2 of S_2 tends to $\delta_2=2\sigma^2T$, so that δ_2/δ_1 tends to 4.0. In the opposite limit, $\sigma T \gg 1$, the output peak-to-peak distance tends to $\delta_{2\text{p.p}}=4\sigma$. Both limits are in agreement with the experimental behavior.

B. Phase modulation

If $\phi(t)$ in Eq. (3) is a bivalued RTN with allowed values $\pm\phi_0$ and mean dwell time T, the power spectrum of the field $b(t)$ is known[5] to be the superposition of a monochromatic part and of a Lorentzian spectrum

$$S_1(\omega-\bar{\omega})=2\pi b_1^2\left[(\cos^2\phi_0)\delta(\omega-\bar{\omega})\right.$$
$$\left.+(\sin^2\phi_0)\frac{2T}{(\omega-\bar{\omega})^2T^2+4}\right]\ . \tag{8}$$

The mean dwell time T controls the width of the Lorentzian part, whereas the phase-jump amplitude ϕ_0 controls the distribution of the integral power between the two contributions. Two representative cases, $\phi_0=\pi/4$ and $\phi_0=\pi/2$, are considered here. According to Eq. (8) the input spectrum $S_1(\omega-\bar{\omega})$ consists of two equal-area contributions for $\phi_0=\pi/4$ and of only the Lorentzian part for $\phi_0=\pi/2$.

To inject a RTN on the phase of a monochromatic radiation, the output signal of the microwave oscillator is passed through an electronic phase shifter, which introduces a phase shift linearly dependent on the external control voltage, with a nominal transition time of 20 nsec. The control input of the phase shifter is driven by one of the RTN voltages of Table I, with amplitude and voltage offset regulated so as to produce the desired amount of phase jump.

In Fig. 3 we report the experimental results obtained for $\phi_0=45°\pm2°$. The spectrum 2(a) is the input field spectrum taken with $T=17.8$ μsec (noise signal E of Table I). Its center peak corresponds to the δ-like contribution to $S_1(\omega-\bar{\omega})$ in Eq. (5), obviously broadened by the frequency resolution of our spectrum analyzer (1 kHz), whereas

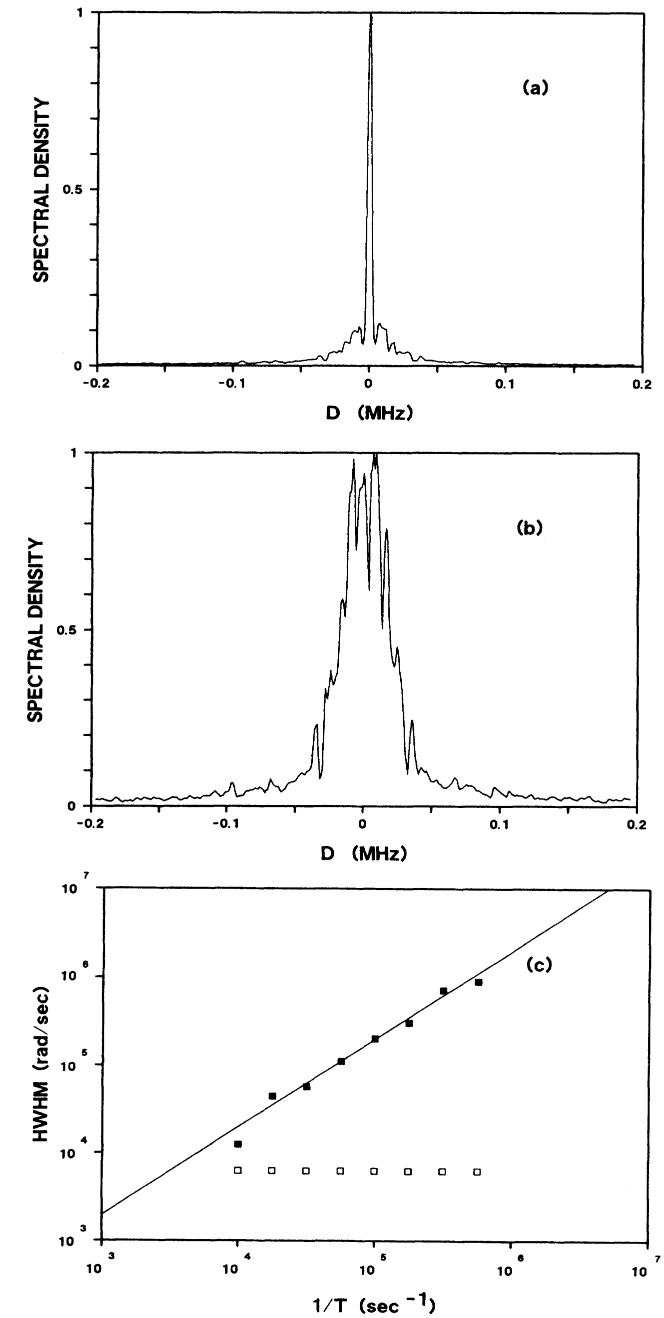

FIG. 3. Telegraph noise of the phase with $\phi_0=45°\pm2°$. (a) Power spectrum, centered at $\bar{\omega}$, of the input field for $T=17.8$ μsec (notice the linear scale). (b) Power spectrum, centered at $2\bar{\omega}$, of the second harmonic emitted by the spin system driven by the field (a). (c) Input (□) and output (■) HWHM, δ_1 and δ_2, respectively, measured by using all the sequences of Table I.

the underlying broad curve corresponds to the Lorentzian part. On increasing T, the relative amplitude of the broad component is found to increase and its width to decrease, until, at long values of T, the two contributions can hardly be distinguished. Note that a linear vertical scale is used in this figure for better evidencing the δ-like contribution and its contrast with the output spectrum.

When the radiation in Fig. 3(a) is used to excite TP transitions in the spin system, the measured SH spectrum, shown in Fig. 3(b), consists of only a broad line with no trace of the monochromatic component of the input spectrum. A similar spectral profile is found in the whole investigated range of T. However, on increasing T, the SH spectrum becomes narrower and narrower, as shown in Fig. 3(c), where the experimental values of δ_2 are plotted versus $1/T$.

The experimental results obtained for $\phi_0=90°\pm2°$ are reported in Fig. 4. In Fig. 4(a) we show a typical spectrum of the input field, as obtained using the noise signal E of Table I ($T=17.8$ μsec). In agreement with Eq. (5), it exhibits only the broad component, whose width δ_1 of $S_1(\omega-\omega)$ depends as $2/T$ on T, as shown in Fig. 4(c). When the radiation in Fig. 4(a) is used to drive the TP-resonant spin system, the power spectrum of the second-order response is found to consist of a very narrow peak superimposed to a much less intense broad line, as in Fig. 4(b); the narrow peak, within our experimental errors, can be taken as a monochromatic component since its width equals the frequency resolution of our spectrum analyzer for any value of T investigated.

The experimental results reported in Figs. 3 and 4 can be explained on the basis of Eq. (5). In fact, according to Eq. (4), for a driving field whose phase is modulated by RTN, the TP Rabi frequency $\omega_R(t)$ is a stochastic process whose phase $\phi_R(t)$ is a RTN with mean dwell time T and a phase-jump amplitude $\phi_{0R}=2\phi_0$. As before, $S_R(\omega)$ can be obtained by rescaling Eq. (8) and we get for the SH spectrum

$$S_2(\omega-2\overline{\omega})=S_0\left[\cos^2(2\phi_0)\delta(\omega-2\overline{\omega})+\frac{2T\sin^2(2\phi_0)}{(\omega-2\overline{\omega})^2T^2+4}\right] \tag{9}$$

with

$$S_0=(\pi\hbar^2N^2\gamma^2/64)\omega_{R0}^2T_2^2\ .$$

For $\phi_0=\pi/4$, namely when the input spectrum [Eq. (8)] has both a δ-like and a Lorentzian part, $S_2(\omega-2\overline{\omega})$ in Eq. (9) consists of only the Lorentzian part, in agreement with the experimental spectrum in Fig. 3(b). Moreover, the HWHM δ_2 of $S_2(\omega-2\overline{\omega})$ is expected from Eq. (9) to vary as $2/T$; the theoretical curve, plotted in Fig. 3(c), well fits the experimental values. The situation is somewhat opposite as regards the case $\phi_0=\pi/2$. Here the input field [Eq. (8)] has only the Lorentzian component, whereas the power spectrum of the second-order response of the system [Eq. (9)] is expected to be δ-like, in agreement with the presence of a narrow center peak in the experimental SH spectrum in Fig. 4(b). This spectral narrowing effect of the system nonlinear response with respect to the driving field can be understood in an intuitive fashion, by considering that the phase jumps with full excursion $2\phi_0=\pi$, which broaden the spectrum of the driving field, yield effectless phase jumps with full excur-

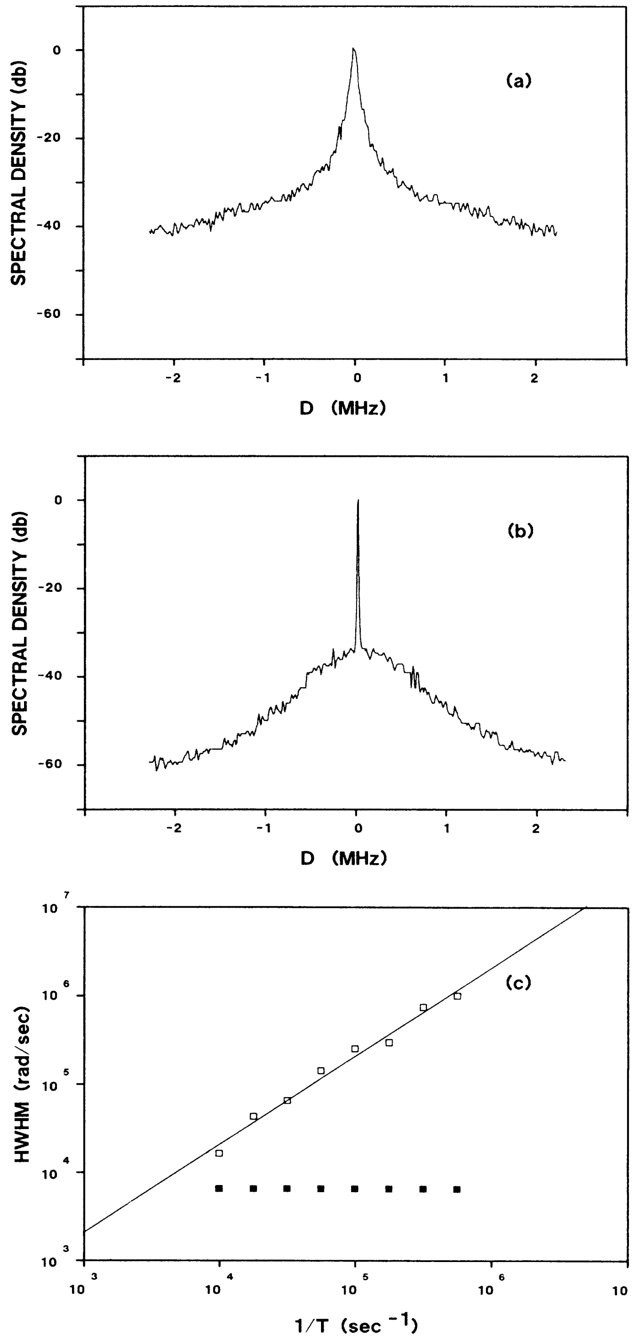

FIG. 4. Telegraph noise of the phase with $\phi_0=90°\pm2°$. (a) Power spectrum, centered at $\overline{\omega}$, of the input field for $T=17.8$ μsec. (b) Power spectrum, centered at $2\overline{\omega}$, of the second harmonic emitted by the spin system driven by the field (a). (c) Input (□) and output (■) HWHM, δ_1 and δ_2, respectively.

sion $2\phi_{R0}=2\pi$ in the TP Rabi frequency; so the second-order response of the system recovers monochromatic properties. Finally, we note that in Fig. 4(b), in addition to the sharp center component, a broad line of minor intensity is visible in the experimental SH spectrum, in contrast with theoretical prediction. We ascribe this discrepancy to the finite width of the cavity modes. In fact, as described in I, both the pump and the detection mode of the resonant bimodal cavity used for the experiments described above have a halfwidth of nearly 400 kHz, so that the spectral wings of the exciting field and of the emitted SH radiation may be altered by the filter action of the cavity. This action manifests itself in a more evident way in the case of the spectrum in Fig. 4(b) for the particular δ-like form of its center part. For this spectrum we have verified that its broad component depends strongly on the tuning of the pump mode, which suggests that it can be considered an experimental artifact.

IV. CONCLUSION

We have reported the experimental realization of nonmonochromatic microwave sources with RTN modulation of phase and frequency. The agreement between experimental and theoretical results indicates that the obtained radiation can be considered an ideal RTN field to a very good approximation in spite of the limited time resolution of the actual RTN sequences used and of their pseudorandom nature. Experiments have been reported in which the obtained RTN radiation is used to induce TP processes in a two-level spin system and its second-order response is investigated in the frequency domain. For a RTN-FM field the output spectrum reproduces roughly the input one but with a larger width. Instead, when a RTN-PM field is used, the form of the output spectrum is different from the input one and in a particular case is δ-like in spite of the finite bandwidth of the driving field spectrum. We emphasize that the experimental results reported here, as well as those in the preceding paper, refer to a case in which the spin system has zero memory, as its relaxation times are much shorter than the correlation time of the input field. Experimental and theoretical work is in progress to extend the present study to the opposite limit, where the coherent effects induced by the fluctuations of the input field parameters cannot be disregarded.

ACKNOWLEDGMENTS

We wish to thank G. Lapis for his technical assistance in cryogenic work. Financial support has been given by Ministero Pubblica Istruzione (national and local funds) and by the National Council of Research (Gruppo Nazionale Struttura della Materia), Rome, Italy.

[1]R. Boscaino and R. N. Mantegna, preceding paper, Phys. Rev. A **40**, 5 (1989).

[2]J. H. Eberly, Phys. Rev. Lett. **37**, 1387 (1976); G. S. Agarwal, *ibid.* **37**, 1383 (1976); S. N. Dixit, P. Zoller, and P. Lambropoulos, Phys. Rev. A **21**, 1289 (1980).

[3]G. N. Van Kampen, *Stochastic Processes in Physics and Chemistry* (North-Holland, Amsterdam, 1981); A. Papoulis, *Probability, Random Variables, and Stochastic Processes,* 2nd ed. (McGraw-Hill, New York, 1984).

[4]Z. Deng and J. H. Eberly, Opt. Commun. **51**, 189 (1984).

[5]J. H. Eberly, K. Wodkiewicz, and B. W. Shore, Phys. Rev. A **30**, 2381 (1984).

[6]K. Wodkiewicz, B. W. Shore, and J. H. Eberly, Phys. Rev. A **30**, 2390 (1984).

[7]B. W. Shore, J. Opt. Soc. Am. B **1**, 176 (1984).

[8]K. Wodkiewicz, B. W. Shore, and J. H. Eberly, J. Opt. Soc. Am. B **1**, 398 (1984).

[9]A. I. Burshtein, A. A. Zharikov, and S. S. Temkin, J. Phys. B **21**, 1907 (1988).

[10]A. I. Burshtein, Zh. Eksp. Teor. Fiz. **48**, 850 (1965) [Sov. Phys.—JETP 21, 567 (1965)]; L. D. Zusman and A. I. Burshtein, *ibid.* **61**, 976 (1972) [*ibid.* **36**, 520 (1972)].

[11]G. Hazak, M. Strauss, and J. Oreg, Phys. Rev. A **32**, 3475 (1985).

[12]H. F. Arnoldus and T. F. George, Phys. Rev. A **35**, 2080 (1987).

[13]H. F. Arnoldus and G. Nienhuis, J. Phys. B **19**, 2421 (1986).

[14]K. Wodkiewicz and J. H. Eberly, Phys. Rev. A **31**, 2314 (1985).

[15]K. Wodkiewicz and J. H. Eberly, J. Opt. Soc. Am. B **3**, 628 (1986).

[16]A. G. Kofman, A. M. Levine, and Y. Prior, Phys. Rev. A **37**, 1248 (1988).

[17]A. G. Kofman, R. Zaibel, A. M. Levine, and Y. Prior, Phys. Rev. Lett. **61**, 251 (1988).

[18]D. S. Elliott, M. W. Hamilton, K. Arnett, and S. J. Smith, Phys. Rev. A **32**, 887 (1985).

[19]M. W. Hamilton, D. S. Elliott, K. Arnett, and S. J. Smith, Phys. Rev. A **33**, 778 (1986).

[20]F. Rohart and B. Macke, Appl. Phys. B **26**, 23 (1981).

[21]R. Boscaino and R. N. Mantegna, Phys. Lett. A **131** 289 (1988); Phys. Rev. A **36**, 5482 (1987).

[22]W. R. Knight and R. Kaiser, J. Magn. Reson. **62**, 65 (1985).

[23]R. Boscaino, I. Ciccarello, C. Cusumano, and M. W. P. Strandberg, Phys. Rev. B **3**, 2675 (1971); F. Persico and G. Vetri, *ibid.* **8**, 3512 (1978).

[24]P. W. Milonni and J. H. Eberly, J. Chem. Phys. **68**, 1602 (1978); R. Boscaino, F. M. Gelardi, and G. Messina, Phys. Rev. B **33**, 3076 (1986); R. Boscaino and G. Messina, Physica C **138**, 179 (1986).

[25]R. Kubo, in *Fluctuations, Relaxation, and Resonance in Magnetic Systems,* edited by D. TerHaar (Oliver and Body, Edinburgh, 1961), pp. 23–66.